nanomaterials

MDPI

Article

Influence of Structural Parameters on Performance of SAW Resonators Based on 128° YX $LiNbO_3$ Single Crystal

Wenping Geng [1,*], Caiqin Zhao [1], Feng Xue [1], Xiaojun Qiao [1], Jinlong He [1], Gang Xue [1], Yukai Liu [1], Huifen Wei [1], Kaixi Bi [1], Linyu Mei [2] and Xiujian Chou [1]

[1] Science and Technology on Electronic Test and Measurement Laboratory, North University of China, Taiyuan 030051, China; s1906211@st.nuc.edu.cn (C.Z.); s1906060@st.nuc.edu.cn (F.X.); xiaojunqiao@nuc.edu.cn (X.Q.); s1906190@st.nuc.edu.cn (J.H.); s1906061@st.nuc.edu.cn (G.X.); sliuyukai@163.com (Y.L.); b1806002@st.nuc.edu.cn (H.W.); bikaixi@nuc.edu.cn (K.B.); chouxiujian@nuc.edu.cn (X.C.)

[2] School of Mechanical Engineering, North University of China, Taiyuan 030051, China; mly81@163.com

* Correspondence: wenpinggeng@nuc.edu.cn; Tel.: +86-0351-3924575

Abstract: The seeking of resonator with high Q and low insertion loss is attractive for critical sensing scenes based on the surface acoustic wave (SAW). In this work, 128° YX $LiNbO_3$-based SAW resonators were utilized to optimize the output performance through IDT structure parameters. Once the pairs of IDTs, the acoustic aperture, the reflecting grid logarithm, and the gap between IDT and reflector are changed, a better resonance frequency of 224.85 MHz and a high Q of 1364.5 were obtained. All the results demonstrate the structure parameters design is helpful for the performance enhancement with regard to SAW resonators, especially for designing and fabricating high-Q devices.

Keywords: surface acoustic wave (SAW); return loss (RL); resonant frequency; resonance device; $LiNbO_3$ single crystal

Citation: Geng, W.; Zhao, C.; Xue, F.; Qiao, X.; He, J.; Xue, G.; Liu, Y.; Wei, H.; Bi, K.; Mei, L.; et al. Influence of Structural Parameters on Performance of SAW Resonators Based on 128° YX $LiNbO_3$ Single Crystal. *Nanomaterials* **2022**, *12*, 2109. https://doi.org/10.3390/nano12122109

Academic Editors: Goran Drazic, Dong-Joo Kim and Shirley Chiang

Received: 29 March 2022
Accepted: 27 May 2022
Published: 19 June 2022

1. Introduction

Recently, surface acoustic wave (SAW) resonators have been playing an important role as key devices in a wide group since the Rayleigh wave was first proposed by Lord Rayleigh in 1885 [1]. The resonators based on SAW technology have been reported in various areas including wideband bandpass filters, high sensitivity sensors, and radio frequency (RF) oscillator [2–4]. The SAW-based devices show noticeable features of high sensitivity and good stability which are closely related with the Q value and insertion loss [5]. A lot of research has been focused on optimizing materials and structure to enhance the performance of the SAW resonators, which has a certain degree of enlightenment for manufacturing high-Q resonators. As shown in the previous literature, Lu et al. extracted a novel electrode-area-weighted (EAW) method of implementing wavelet transform processor (WTP) with SAW device based on X-112°Y $LiTaO_3$ [6]. A. J. Vigil et al. presented approaches for SAW filter design used in pulsed Quadrature Binary Modulation (QBM) systems with split interdigital transducer (IDT) [7]. Ye et al. reported YZ-cut $LiNbO_3$ is suitable for the fabrication of SAW temperature sensors for its higher sensitivity and larger Q factor [8]. However, the electromechanical coupling coefficients (K^2) and phase velocity of X-112°Y $LiTaO_3$ and YZ-cut $LiNbO_3$ are limited; moreover, the temperature stability of them is relatively poor [9]. Regarding these aspects, 128° YX $LiNbO_3$ is a better substrate choice to be utilized for SAW resonator, due to extremely low sound loss and piezoelectric properties. Inspired by the previous work, improving the IDT structure of 128° YX $LiNbO_3$-based SAW resonators is meaningful for high Q value and low insertion of SAW resonators.

In this work, 128° YX $LiNbO_3$-based SAW resonators were designed and fabricated with different parameters based on equivalent circuit model. Vector network analyzer

(VNA) and RF probe station were used to test the signal of the manufactured devices. The comparison and analysis of the influence of different parameters on SAW resonant is performed through experiment results and the SAW resonator with Q 1364.5 is obtained that could be used for high performance SAW devices preparation.

2. Experimental

2.1. Design and Materials of SAW Resonator

The operating principle of SAW devices is based on the direct piezoelectric effect and inverse piezoelectric effect of piezoelectric substrate materials. It could be seen as an equivalent circuit when the device is resonating, which converts crystal substrate and device parameters to RCL circuit shown in Figure 1b. Where C_0 is static capacitance, R_a is radiation resistance, C_S is equivalent dynamic capacitance, L_S is equivalent dynamic inductance, and R_q is equivalent dynamic resistance.

$$C_0 = N_p(\varepsilon_r\varepsilon_0 + \varepsilon_0)W \tag{1}$$

where N_p is pairs of IDTs, W is acoustic aperture, ε_0 is dielectric constant under vacuum, and ε_r is relative dielectric constant of piezoelectric substate. C_0, R_a, C_s and so on

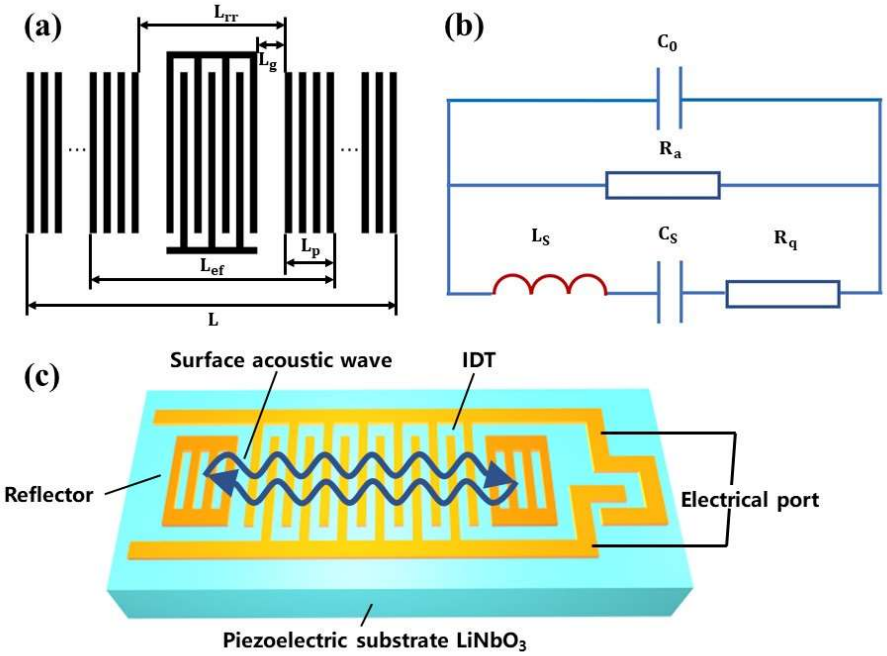

Figure 1. (**a**) Parameter diagram, (**b**) general equivalent circuit diagram, and (**c**) diagram of single port SAW resonator.

The theoretical calculation formula of R_a is as follows:

$$R_a = \frac{1}{(8K^2 f_0 C_p W N_p^2)} \tag{2}$$

where K^2 is electromechanical coupling coefficient of piezoelectric materials, and f_0 is the resonant frequency of SAW devices.

$$f_0 = \frac{c}{\lambda} = \frac{c}{p_i} \tag{3}$$

$$\lambda = 2(a + b) \tag{4}$$

where f_0 is the resonant of the SAW device, c is the velocity of sound in the piezoelectric materials, λ is the wavelength of the SAW, p_i is the periodicity of IDTs, a and b represent line width and gap of the IDT, respectively.

The theoretical calculation formula of R_q is as follows:

$$R_q = R_a[\frac{(1-|\Gamma|)}{(2|\Gamma|)}] \tag{5}$$

where Γ is reflection coefficient of reflector, Z_m is acoustic impedance of the substrate coated surface, Z_0 is acoustic impedance of the substrate free surface, ΔZ is acoustic impedance discontinuity value of reflector, and N_g is reflecting grid logarithm.

$$|\Gamma| = \left|\frac{\left(\frac{Z_m}{Z_0}\right)^{2N_g}-1}{\left(\frac{Z_m}{Z_0}\right)^{2N_g}+1}\right| \tag{6}$$

$$\frac{Z_m}{Z_0} = 1+\Delta Z \tag{7}$$

The theoretical calculation formula of L_S is as follows:

$$L_S = R_a\cdot[\frac{L_{ef}}{(4f_0|\Gamma|\lambda_0)}] \tag{8}$$

$$L_{ef} = L_{rr}+2L_p \tag{9}$$

$$L_{rr} = N_p(a+b)+2L_g = N_p(\frac{\lambda_0}{2})+2L_g \tag{10}$$

$$L_p = \frac{\lambda_0}{4|\Delta Z|} \tag{11}$$

where L_{ef} is effective cavity length, L_{rr} is the distance between the two reflectors, L_p is penetration depth of SAW energy, and L_g is the gap between interdigital transducer and reflector.

The theoretical calculation formula of C_S is as follows:

$$C_S = \frac{1}{[(2\pi f_0)^2 L_S]} \tag{12}$$

According to the above-mentioned equivalent circuit model and parameters of the theoretical formula, structure parameters and material characteristic parameters are closely related.

For several important parameters, the design parameters are as presented in Table 1.

Table 1. Main design parameters of surface acoustic wave resonator [10].

Design Parameter	Value
a = b	3 μm, 4 μm, 5 μm
N_p	30, 50, 70, 90
W	50 λ, 75 λ, 100 λ
L_g (short-circuit reflector)	20, 44, 116
L_g (open-circuit reflector)	24, 48, 120
N_g	50, 100, 200, 250

There are two main types of reflectors: short-circuit reflector and open-circuit reflector [11]; ΔZ is different for $LiNbO_3$, as shown in the Equation (13):

$$L_g \begin{cases} \left(n - \frac{1}{2}\right)\frac{\lambda}{2} (\Delta Z < 0) \\ n\frac{\lambda}{2} (\Delta Z > 0) \end{cases} \quad (13)$$

As for short-circuit reflector $\Delta Z < 0$, and open-circuit reflector $\Delta Z > 0$. Where n is an integer, 3, 6, 15.

Electrode material is also a vital factor for propagation of SAW. The selection of electrode material requires: substrate materials, device cycle, etc. Aluminum, copper, platinum, and gold are typical metal materials for preparation of SAW devices. Gold not only has good ductility and high temperature tolerance, but gold deposition is compatible with other micro-electromechanical systems (MEMS) [12] technology. Therefore, gold is chosen as the electrode material, which is 120 nm thick.

The SAW resonators have been successfully fabricated by ion beam etching (IBE). Pretreatment is carried out primarily for cleaning the substrate, generally adopting the following processes: organic cleaning, acid picking, alkali washing. Organic matter on the surface of the $LiNbO_3$ is removed by organic cleaning. The purpose of acid picking is to clean the metal particle, and the use of the alkali washing is to wipe off the acid solution residue. Then magnetron sputtering is utilized for coating the metal film. Traditional photolithography is performed on coated wafers. Finally, an IBE procession is used for removing the rest of metal. Figure 2a shows the scanning electron microscopy (SEM) image of the complete SAW resonator and Figure 2b–d exhibit the SEM images of IDTs structure with different resolutions.

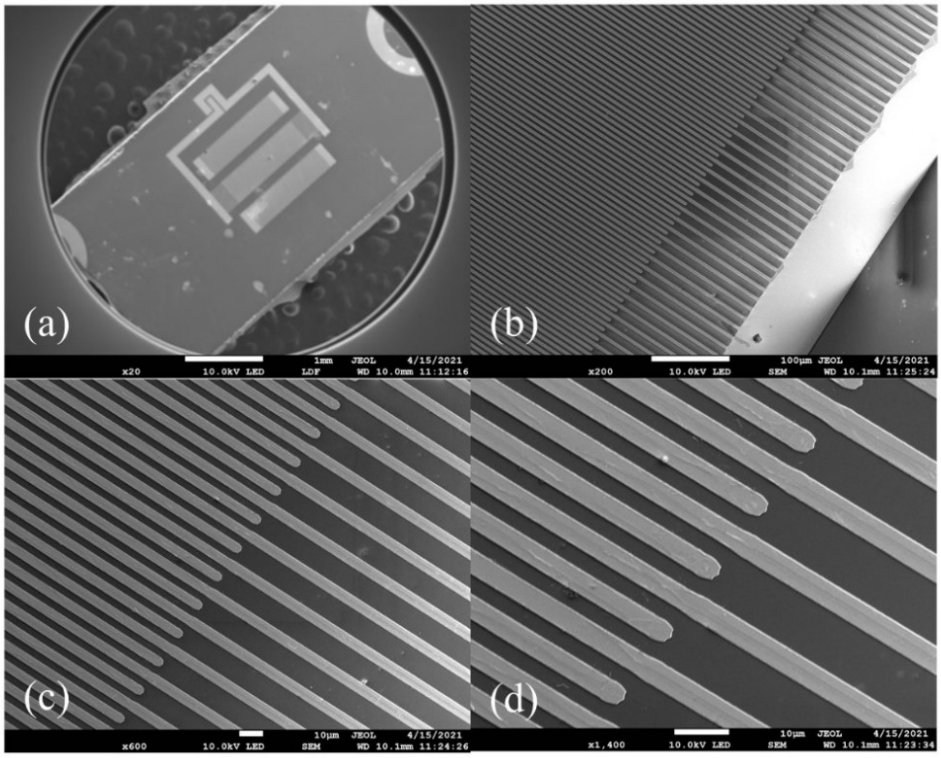

Figure 2. (**a**) SEM image of SAW resonator, (**b**) 200 times, (**c**) 600 times, and (**d**) 1400 times magnification of IDTs structure with a width of 4 μm.

2.2. Characterization and Testing Instrumentation

Figure 3a shows a SAW resonator test platform containing VNA and RF probe station. Microwave network parameters are tested by VNA which is Agilent E5071C made in

Malaysia. RF probe station is unified with Ground-Signal-Ground (GSG) probe that has solved many measurement problems by its multiple functions and pinpoint accuracy. Figure 3b shows the image of GSG probe test under a charge coupled device (CCD) microscope.

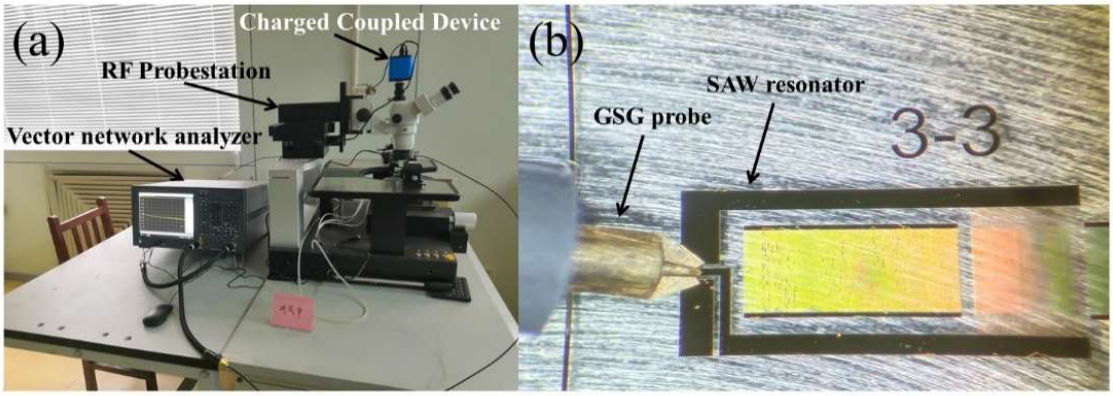

Figure 3. (**a**) Photo of the testing platform, (**a**) RF Probe station connected to Agilent E5071C vector network analyzer, (**b**) GSG probe with SAW resonator.

The S11 parameter is defined as the rate of reflected power and incident power of the device which effectively captures a series of physical processes containing the acoustoelectric conversion and spreads the reflection of SAW [13,14]. The signal output and input of single-ended resonator are accomplished by the same port owing to its performance, which could be characteristic of S11 parameter. In the following section SAW resonator test results are represented by its S11 parameter.

3. Results and Discussions

According to the S11 characteristic curves in Figure 4a, the center frequencies of the SAW resonators with wavelength 12, 16, and 20 μm on 128° YX $LiNbO_3$ substrate are 178.65, 222.5, and 295 MHz, respectively. The wave velocity of the 128° YX $LiNbO_3$ is about 3540~3573 m/s based on the Equation (3). The periodicity of IDTs p_i is a key factor for the resonance frequency of the SAW devices, that directly determines the resonant frequency of the SAW device [15]. To achieve a high-performance SAW device, two parameters, v and p_i should be well considered.

The pairs of IDTs are inversely proportional to bandwidth, which means $N_p \propto 1/f_{BW}$, and a smaller bandwidth f_{BW} is beneficial to improving the Q value of the device. As shown in Figure 4b, the S11 parameters of the SAW resonators with IDT are 30, 50, 70, and 90 pairs, respectively. The sidelobe of the S11 curves are suppressed and the harmonic peaks are steeply increased with the pairs of IDTs changing from 30 to 90 pairs so that the S11 gradually increases in the range of 10.725 dB. The reasonableness of N_p should be measured comprehensively by size and difficulty of process preparation.

According to the Equation (1), an increase in W causes an increase in C_0, which means the coupling is stronger. It is beneficial to reduce the insertion loss and improve the Q value. Figure 4c shows that the S11 parameters curves of SAW resonators with W are 50 λ, 75 λ, and 100 λ, respectively, which have the same N_p i.e., 90. The result has an apparent tendency to increase with an increase in W, which varied from −17.38 dB to −26.32 dB. Figure 4d shows SAW resonators with N_p of 30 and with W of 50 λ, 75 λ, and 100 λ, respectively; it can be seen that the sidelobe of the devices are suppressed with an increase of W. In brief, whether to add N_p or increase W will greatly enhance the performance of the SAW resonators. An increase in W is accompanied by the increase in device volume. On the contrary, the diffraction effect of surface acoustic wave will be aggravated [16].

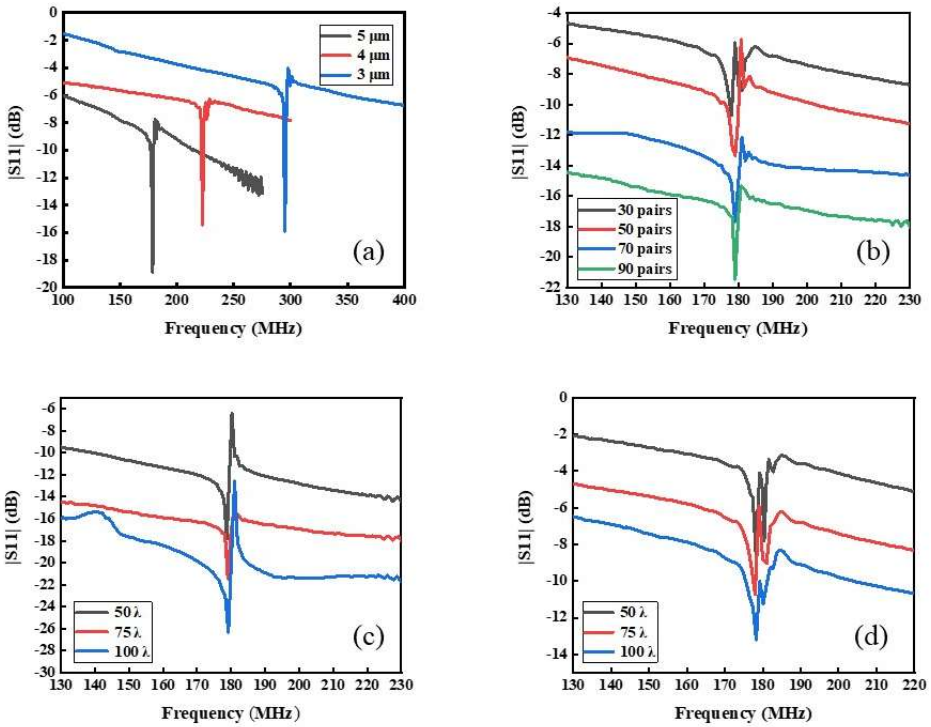

Figure 4. (**a**) Centre frequency of IDT with different λ, (**b**) S11 parameters curves of IDT with different pairs N_p. S11 parameters curves of IDT with different acoustic aperture W, (**c**) each of these devices has 50 pairs of IDTs, (**d**) each of these devices has 30 pairs of IDTs. 5 μm.

Ignoring the second-order effect, the no-load Q value of the resonator can be approximated as in Equation (14).

$$Q = \frac{\pi L_{ef}}{(1 - |\Gamma|)\lambda} \tag{14}$$

It can be seen from Equation (14) that the L_{ef} appropriate increase is conducive to improving the Q value. Figure 5a shows L_g = 22, 44, and 116 μm, when L_g = 44 μm, the S11 parameter is the sharpest among them, which is −18.9 dB and its center frequency is 223.5 MHz, besides they have short-circuited reflectors. In addition, open-circuit reflectors are shown in Figure 5b. The S11 parameter of the resonator when L_g = 48 μm is −19.78 dB which greatly exceeds L_g = 24 and 120 μm and center frequency is 224 MHz. According to the above analysis, appropriately increasing L_g could improve Q value. The type of reflector has little influence on the performance of the SAW resonator is yet to be researched. Appropriate L_g keeps incident and reflected waves overlay on each other to form standing waves, that is Bragg reflection [17]. The center of the interdigital is set on the standing wave peak to enhance the electromechanical coupling efficiency [18].

Reflection coefficient has a great influence on the Q value [19], and it is positively correlated with N_g. It should be satisfied in actual design that $N_g|\Delta Z/Z| = 3$–4. As shown in Figure 5c, the performance of the device is better when N_g is 100, that is S11 is −16.054 dB. When N_g is 50, 200, 250, the performance of the device is not an obvious improvement.

Group delay algorithm is adopted to calculate Q value [20,21], according to the Equation (15):

$$Q(f) = \frac{2\pi f \cdot \tau(f) \cdot |\Gamma(f)|}{(1 - |\Gamma(f)|^2)} \tag{15}$$

where $\tau(f)$ is ground delay coefficient and $|\Gamma(f)|$ is the amplitude of S11 [20]. The measured types for all structure SAW resonators are quite adequate for several practical designs when the pairs of IDTs are 90, the acoustic aperture is 100 λ, the L_g is 44 μm, and the N_g is 100. The resonator shows great Q value as high as 1364.5 shown in Figure 5d, which is beneficial to manufacture highly sensitive and greater sensing sensor.

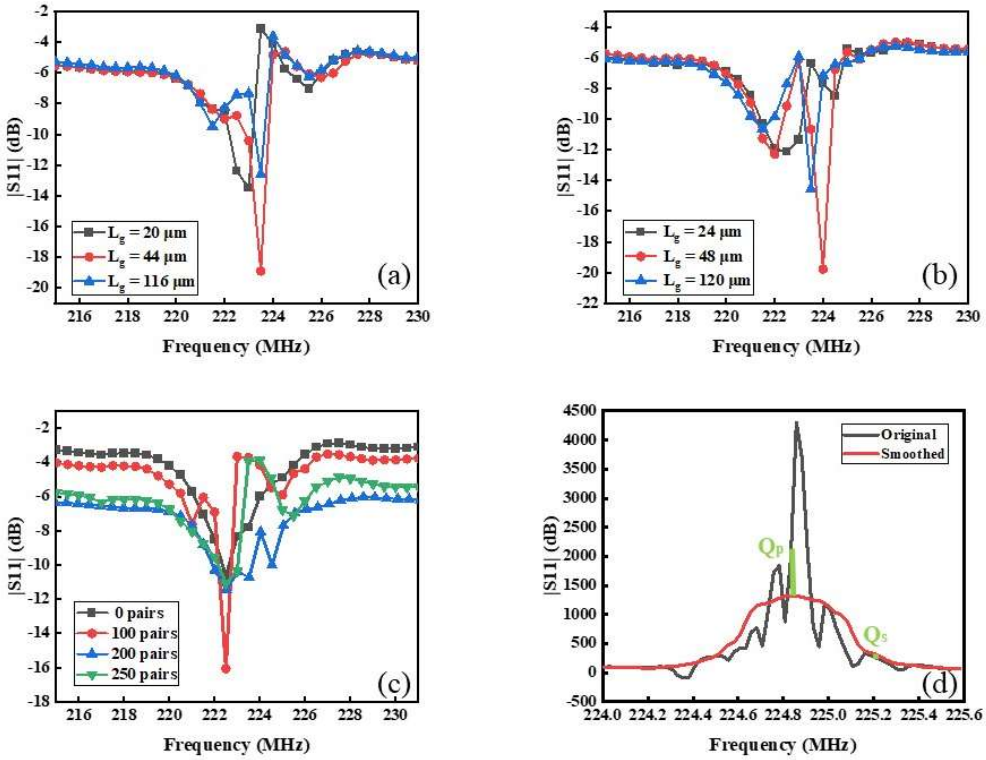

Figure 5. S11 parameter curves of the SAW devices with three kinds of L_g, (**a**) short-circuit reflector and (**b**) open-circuit reflector. (**c**) S11 parameter curves of the SAW devices with four kinds of reflecting grid logarithm. (**d**) The group delay algorithm calculates Q value.

SAW resonators' performances in previous work are summarized in Table 2, showing resonance frequency and Q value. The resonator presents the advantage of having a high Q value 1364.5, which is essential for fabricating a SAW load sensor with higher sensitivity and a larger sensing range.

Table 2. Comparison works on performance of SAW resonators.

Piezoelectric Substrate	f (MHz)	Q Value
AlN/Al_2O_3 [22]	688.75	1082
$Sc_{0.23}Al_{0.77}N/Al_2O_3$ [23]	1910	659
$LiNbO_3$ [24]	150	1150
Quartz [25]	433.05–434.79	8000
ZnO/6H-SiC [26]	688	1080
128° YX $LiNbO_3$ (this work)	224.85	1364.5

4. Conclusions

In conclusion, a high-Q 1364.5 SAW resonator based on 128° YX $LiNbO_3$ is obtained through a variety of SAW resonators with selection and optimization of structural parameters. The period of the IDT and parameter of materials determines the resonant frequency of SAW resonators. SAW resonators working on a central frequency of 178.65, 222.5, and 295 MHz were fabricated. The SAW resonators were fabricated with 30, 50, 70, and 90 pairs of IDTs, exhibiting interesting behavior to Q value. The maximum S11 shift was 10.725 dB. SAW resonators with acoustic aperture of 50 λ, 75 λ, and 100 λ were prepared and tested. Diffraction can be effectively suppressed by increasing the aperture. It is suggested that the reasonable gap between IDT and reflector was conductive to the generation of standing waves. Meanwhile, the reflecting grid logarithm increase would increase the reflection coefficient. However, the style of the reflector was not a key factor for Q value. IBE is utilized to prepare the SAW resonators and the VNA with RF probe station was used

for testing them. It is suggested from the experimental results that combining typical equivalent circuit model and MEMS processing technology achieved optimal performance of SAW resonator that is of great significant for highly sensitive SAW sensors.

Author Contributions: Conceptualization, W.G. and C.Z.; methodology, C.Z.; validation, W.G., C.Z. and F.X.; investigation, X.Q., J.H. and G.X.; resources, Y.L. and H.W.; data curation, C.Z.; writing—original draft preparation, C.Z.; writing—review and editing, W.G., K.B. and L.M.; supervision, X.C.; project administration, K.B., W.G. and X.C.; funding acquisition, W.G., L.M. and X.C. All authors have read and agreed to the published version of the manuscript.

Funding: This research was funded by the National Natural Science Foundation of China [grant numbers 62171415, 51975541], Key R&D Projects of Shanxi Province [grant number 20201101015].

Institutional Review Board Statement: Not applicable.

Informed Consent Statement: Not applicable.

Data Availability Statement: The data presented in this study are available in this article.

Conflicts of Interest: The authors have no conflict of interest to declare.

References

1. Rayleigh, L. On waves propagated along the plane surface of an elastic body. In *Proceedings of the London Mathematical Society*; Oxford University Press: Oxford, UK, 1885.
2. Lu, X.; Mouthaan, K.; Soon, Y.T. Wideband Bandpass Filters With SAW-Filter-Like Selectivity Using Chip SAW Resonators. *IEEE Trans. Microw. Theory Tech.* **2014**, *62*, 28–36. [CrossRef]
3. Nordin, A.N.; Zaghloul, M. RF oscillator implementation using integrated CMOS surface acoustic wave resonators. *Analog Integr. Circuits Signal Process.* **2011**, *68*, 33–42. [CrossRef]
4. Canabal, A.; Davulis, P.; Harris, G.; da Cunha, M.P. High-temperature battery-free wireless microwave acoustic resonator sensor system. *Electron. Lett.* **2010**, *46*, 471–472. [CrossRef]
5. Wang, C.; Wang, Y.; Zhang, S.Y.; Fan, L.; Shui, X.J.J.S.; Chemical, A.B. Characteristics of SAW hydrogen sensors based on InOx/128°YX-$LiNbO_3$ structures at room temperature. *Sens. Actuators B* **2012**, *173*, 710–715. [CrossRef]
6. Lu, W.; Zhu, C.; Liu, Q.; Zhang, J. Implementing wavelet inverse-transform processor with surface acoustic wave device. *Ultrasonics* **2013**, *53*, 447–454. [CrossRef] [PubMed]
7. Vigil, A.J.; Madjid, D.C.M.; Belkerdid, A. Design of SAW FIR Filters for Quadrature Binary Modulation Systems. *IEEE Trans. Ultrason. Ferroelectr. Freq. Control* **1993**, *40*, 504. [CrossRef]
8. Ye, X.; Wang, Q.; Fang, L.; Wang, X.; Liang, B. Comparative Study of SAW Temperature Sensor Based on Different Piezoelectric Materials and Crystal Cuts for Passive Wireless Measurement. In *Sensors, Proceedings of the 2010 IEEE, Waikoloa, HI, USA, 1–4 November 2010*; IEEE: New York, NY, USA, 2010.
9. Jiang, H.; Lu, W.K.; Shen, S.G.; Xie, Z.G. Materials, Study of a Low Insertion Loss SAW Filter with SPUDT Structure Using YZ-$LiNbO_3$. In *Applied Mechanics and Materials*; Trans Tech Publications Ltd.: Schwyz, Switzerland, 2013; Volume 251, pp. 139–142.
10. Bell, D.T.; Li, R.C. Surface-Acoustic-Wave Resonators. *Proc. IEEE* **1976**, *64*, 711–721. [CrossRef]
11. Wang, W.; Lee, K.; Woo, I.; Park, I.; Yang, S. Optimal design on SAW sensor for wireless pressure measurement based on reflective delay line. *Sens. Actuators A Phys.* **2007**, *139*, 2–6. [CrossRef]
12. Lin, M.-T.; El-Deiry, P.; Chromik, R.R.; Barbosa, N.; Brown, W.L.; Delph, T.J.; Vinci, R.P. Temperature-dependent microtensile testing of thin film materials for application to microelectromechanical system. *Microsyst. Technol.* **2006**, *12*, 1045–1051. [CrossRef]
13. Bu, G.; Ciplys, D.; Shur, M.; Schowalter, L.; Schujman, S.; Gaska, R. Surface Acoustic Wave Velocity in Single-Crystal AlN Substrates. *IEEE Trans. Ultrason. Ferroelectr. Freq. Control* **2006**, *53*, 251–254. [CrossRef]
14. Sha, G.; Harlow, C.; Chernatynskiy, A.; Daw, J.; Khafizov, M. In-situ measurement of irradiation behavior in $LiNbO_3$. *Nucl. Instrum. Methods Phys. Res. Sect. B* **2020**, *472*, 46–52. [CrossRef]
15. Zhou, P.; Chen, C.; Wang, X.; Hu, B.; San, H. 2-Dimentional photoconductive MoS_2 nanosheets using in surface acoustic wave resonators for ultraviolet light sensing. *Sens. Actuators A Phys.* **2018**, *271*, 389–397. [CrossRef]
16. Lu, W.; Gao, L.; Zhang, J. A novel electrode-area-weighted method of implementing wavelet transform processor with surface acoustic wave device. *Int. J. Circuit Theory Appl.* **2016**, *44*, 2134–2146. [CrossRef]
17. Astley, M.R.; Kataoka, M.; Schneble, R.J.; Ford, C.J.B.; Barnes, C.H.W.; Anderson, D.; Jones, G.A.C.; Beere, H.E.; Ritchie, D.A.; Pepper, M. Examination of surface acoustic wave reflections by observing acoustoelectric current generation under pulse modulation. *Appl. Phys. Lett.* **2006**, *89*, 132102. [CrossRef]
18. Rummel, B.D.; Miroshnik, L.; Patriotis, M.; Li, A.; Sinno, T.R.; Henry, M.D.; Balakrishnan, G.; Han, S.M. Imaging of surface acoustic waves on GaAs using 2D confocal Raman microscopy and atomic force microscopy. *Appl. Phys. Lett.* **2021**, *118*, 031602. [CrossRef]

19. Darinskii, A.; Weihnacht, M.; Schmidt, H. Anisotropy effects in the reflection of surface acoustic waves from obstacles. *IEEE Trans. Ultrason. Ferroelectr. Freq. Control* **2013**, *60*, 235–242. [CrossRef]
20. Ruby, R.; Parker, R.; Feld, D. Method of Extracting Unloaded Q Applied Across Different Resonator Technologies. In Proceedings of the 2008 IEEE Ultrasonics Symposium, Beijing, China, 2–5 November 2008; pp. 1815–1818.
21. Feld, D.A.; Parker, R.; Ruby, R.; Bradley, P.; Dong, S. After 60 years: A new formula for computing quality factor is warranted. In Proceedings of the 2008 IEEE Ultrasonics Symposium, Beijing, China, 2–5 November 2008; pp. 431–436.
22. Ai, Y.; Yang, S.; Cheng, Z.; Zhang, L.; Jia, L.; Dong, B.; Wang, J.; Zhang, Y. Enhanced performance of AlN SAW devices with wave propagation along the $\langle 11-20 \rangle$ direction on c-plane sapphire substrate. *J. Phys. D Appl. Phys.* **2019**, *52*, 215103. [CrossRef]
23. Ding, A.; Kirste, L.; Lu, Y.; Driad, R.; Kurz, N.; Lebedev, V.; Christoph, T.; Feil, N.M.; Lozar, R.; Metzger, T.; et al. Enhanced electromechanical coupling in SAW resonators based on sputtered non-polar Al0.77Sc0.23N 1120 thin films. *Appl. Phys. Lett.* **2020**, *116*, 101903. [CrossRef]
24. Song, Y.-H.; Lu, R.; Gong, S. Analysis and Removal of Spurious Response in SH0 Lithium Niobate MEMS Resonators. *IEEE Trans. Electron. Devices* **2016**, *63*, 2066–2073. [CrossRef]
25. Moutoulas, E.; Hamidullah, M.; Prodromakis, T. Surface Acoustic Wave Resonators for Wireless Sensor Network Applications in the 433.92 MHz ISM Band. *Sensors* **2020**, *20*, 4294. [CrossRef]
26. Li, Q.; Qian, L.; Fu, S.; Song, C.; Zeng, F.; Pan, F. Characteristics of one-port surface acoustic wave resonator fabricated on ZnO/6H-SiC layered structure. *J. Phys. D Appl. Phys.* **2018**, *51*, 145305. [CrossRef]